International Journal of Nanomedicine

Dovepress

open access to scientific and medical research

Open Access Full Text Article

ORIGINAL RESEARCH

pH-Responsive Block Copolymer Micelles of Temsirolimus: Preparation, Characterization and Antitumor Activity Evaluation

Ling Wang[1–3,*], Fangqing Cai[3,*], Yixuan Li[3,*], Xiaolan Lin[3], Yuting Wang[3], Weijie Liang[3], Caiyu Liu[4], Cunze Wang[3], Junshan Ruan[1–3]

[1]School of Pharmacy, Fujian Medical University, Fuzhou University Affiliated Provincial Hospital, Fuzhou, Fujian Province, People's Republic of China; [2]Molecular Biology Laboratory of Traditional Chinese Medicine, Fujian Provincial Hospital, Fuzhou, Fujian Province, People's Republic of China; [3]School of Pharmacy, Fujian Medical University, Fuzhou, Fujian Province, People's Republic of China; [4]School of Pharmacy, Fujian University of Traditional Chinese Medicine, Fuzhou, Fujian Province, People's Republic of China

*These authors contributed equally to this work

Correspondence: Junshan Ruan, School of Pharmacy, Fujian Medical University, Fuzhou University Affiliated Provincial Hospital, 134 Dongjie, Fuzhou, 350001, People's Republic of China, Tel +86 591-88216343, Fax +86 591-87532356, Email ruanjunshan@163.com

Purpose: Renal cell carcinoma (RCC) is the most common and lethal type of urogenital cancer, with one-third of new cases presenting as metastatic RCC (mRCC), which, being the seventh most common cancer in men and the ninth in women, poses a significant challenge. For patients with poor prognosis, temsirolimus (TEM) has been approved for first-line therapy, possessing pharmacodynamic activities that block cancer cell growth and inhibit proliferation-associated proteins. However, TEM suffers from poor water solubility, low bioavailability, and systemic side effects. This study aims to develop a novel drug formulation for the treatment of RCC.

Methods: In this study, amphiphilic block copolymer (poly(ethylene glycol) monomethyl ether-poly(beta-amino ester)) (mPEG-PBAE) was utilized as a drug delivery vehicle and TEM-loaded micelles were prepared by thin-film hydration method by loading TEM inside the nanoparticles. Then, the molecular weight of mPEG-PBAE was controlled to make it realize hydrophobic–hydrophilic transition in the corresponding pH range thereby constructing pH-responsive TEM-loaded micelles. Characterization of pH-responsive TEM-loaded nanomicelles particle size, potential and micromorphology while its determination of drug-loading properties, in vitro release properties. Finally, pharmacodynamics and hepatorenal toxicity were further evaluated.

Results: TEM loading in mPEG-PBAE increased the solubility of TEM in water from 2.6 μg/mL to more than 5 mg/mL. The pH-responsive TEM-loaded nanomicelles were in the form of spheres or spheroidal shapes with an average particle size of 43.83 nm and a Zeta potential of 1.79 mV. The entrapment efficiency (EE) of pH-responsive TEM nanomicelles with 12.5% drug loading reached 95.27%. Under the environment of pH 6.7, the TEM was released rapidly within 12 h, and the release rate could reach 73.12% with significant pH-dependent characteristics. In vitro experiments showed that mPEG-PBAE preparation of TEM-loaded micelles had non-hemolytic properties and had significant inhibitory effects on cancer cells. In vivo experiments demonstrated that pH-responsive TEM-loaded micelles had excellent antitumor effects with significantly reduced liver and kidney toxicity.

Conclusion: In conclusion, we successfully prepared pH-responsive TEM-loaded micelles. The results showed that pH-responsive TEM-loaded micelles can achieve passive tumor targeting of TEM, and take advantage of the acidic conditions in tumor tissues to achieve rapid drug release.

Keywords: renal cell carcinoma, drug delivery, pH-responsive, mPEG-PBAE, nanomicelles

Introduction

Renal cell carcinoma (RCC) is highly aggressive,[1] with insidious early symptoms and poor treatment leading to high mortality. The incidence of non-clear cell RCC (nccRCC) is no more than 8%-20%.[2] Its rarity and poor prognosis have

Received: 20 March 2024
Accepted: 3 September 2024
Published: 23 September 2024

made it difficult to determine the best treatment option, and current treatments include surgery and targeted therapy.[3] In recent years, tyrosine kinase inhibitors (TKIs) targeting vascular endothelial growth factor receptor (VEGFR) pathways, such as sunitinib,[4,5] and sorafenib,[6,7] and mammalian target of rapamycin (mTOR) inhibitors, such as temsirolimus (TEM)[8,9] and everolimus,[10,11] have been developed for the treatment of metastatic RCC (mRCC).[12] TEM shrinks tumors and slows cancer progression,[13] and has been shown to be effective in advanced RCC.

In a large Phase III clinical study, patients with TEM had longer overall, progression-free survival ($p < 0.001$) and fewer patients with serious adverse events ($p = 0.02$) as compared to patients with interferon alone.[8] VEGFR-TKI are approved for the treatment of patients with mRCC, but resistance usually occurs after 6–11 months of treatment, and sequential therapy with mTOR inhibitors is usually used for patients who have failed VEGFR-TKI therapy. It has been shown that after sequential treatment with mTOR inhibitors, patients are re-sensitized to VEGFR-TKI, prolonging the therapeutic benefit for patients.[14,15] mTOR specifically acts on FK506-binding protein targets to generate protein-drug complexes. Binding of mTOR to this complex will result in the blockage of the phosphorylation process of protein expression-associated factors downstream of the PI3K/Akt/mTOR pathway, such as eukaryotic translation initiation factor 4E-binding protein 1 and p70S6 kinase, which inhibits the translation of key proteins and causes the cell cycle to be blocked in the G_1 phase.[12,16] mTOR targeting by TEM also inhibits proteins that regulate angiogenesis and the production of growth-stimulating factors.[17,18] In vitro studies have shown that TEM can regulate the translation of HIF-1α and HIF-2α and the production of the angiogenic factor VEGF.[19,20] Moreover, unlike antiangiogenic agents, mTOR mainly acts in tumor cells.[21] TEM decreased PD1 expression of $CD8^+$ T cells and early-stage MDSC and increased interferon and tumor necrosis factor production.[22] The study indicated that TEM was expected to offer the best outcome with immunomodulators in RCC.[23]

However, the efficacy and safety of TEM is severely limited by the deficiencies in solubility and bioavailability. TEM is virtually insoluble in water, and thus poorly absorbed and distributed in vivo. The original developer of TEM used Tween 80 and organic solvents to dissolve the drug and overcome the limited solubility of it, which caused greater irritation during intravenous injection, thus decreasing the patient's compliance. Anhydrous citric acid and vitamin E were added to the diluent as stabilizer and antioxidant, respectively, which increased the cost of drug packaging and transportation. Moreover, mTOR is widely distributed, and the low tissue targeting of the inhibitor is prone to increase the risk of infection, gastrointestinal symptoms and changes in blood glucose levels, and other potential side effects.

To address these challenges, various stimuli-responsive polymeric micelles (PMs) have been developed. Temperature,[24–27] pH,[28–34] light,[35–37] electric,[38,39] enzyme,[40–42] etc. are the driving forces for controlling drug release. Poly(ethylene glycol) monomethyl ether-poly (beta-amino ester) (mPEG-PBAE) diblock copolymer, as a drug delivery material, can take advantage of the acidic conditions in tumor tissues to achieve the rapid release of drugs, and its high biocompatibility is conducive to the reduction of irritation and damage of organisms, thus reducing the toxicity and side effects.[43] In addition, the hydrophobic chain segment poly(beta-amino ester) is biocompatible and degradable in vivo, and its tertiary amine group can be protonated in the acidic microenvironment of tumor tissues to produce a hydrophobic–hydrophilic transition of the chain segment, and the hydrophobic segment breaks to enable rapid drug release. This study aimed to develop and optimize a preparation of mPEG-PBAE, relying on the flexibility and controllability of molecular weight and block ratio of the block copolymer material poly (ethylene glycol)-poly(beta-amino ester) and conducted comprehensive characterizations to assess the particle size, distribution, stability, and pH-responsive range of the TEM-loaded nanomicelles. In vitro release studies and in vivo experiments were conducted to evaluate the anti-RCC activity of TEM-loaded micelles.

Materials and Methods

Materials

TEM (standard, 99% purity) purchased from AbMole (USA); TEM was bought from Shanghai Hanxiang Biotechnology Co., Ltd. (Shanghai, China); Acetonitrile (ACN) (chromatography grade), methanol (MeOH) (chromatography grade), acryloyl chloride, n-hexane, 4-methylpiperidine, 1,6-hexanediol diacrylate (1,6-HDDA), anhydrous calcium chloride and trifluoroacetic acid (TFA) were purchased from Shanghai Maclean's Biochemical Technology Co., Ltd. (Shanghai, China); poly(ethylene glycol)monomethyl ether (mPEG, Mw = 2000) from Sigma-Aldrich (USA); Triethylamine,

methylene chloride, hydrochloric acid, chloroform are from Shanghai Lingfeng Chemical Reagent Co., Ltd. (Shanghai, China); 1,3-Bis(4-piperidyl)propane comes from Shanghai Yuanye Biotechnology Co., Ltd. (Shanghai, China); Anhydrous ether was purchased from Yonghua Chemical Co., Ltd. (China); MeOH from Thermo (USA); Dimethyl sulfoxide (DMSO) from Beijing Solaibao Technology Co., Ltd. (Beijing, China); RPMI 1640 medium, phosphate-buffered solution (PBS), 0.25% trypsin/EDTA solution, fetal bovine serum (FBS) and Enhanced Cell Counting Kit-8 (CCK-8) were all from Dalian Meilun Biotechnology Co., Ltd. (Dalian, China); Coumarin-6 was purchased from Shanghai Aladdin Biochemical Technology Co., Ltd. (Shanghai, China). 786-O cells in our study were purchased from Prosel Life Science and Technology Co., Ltd (Wuhan, China).

Establishment of the Detection Methodology for TEM

Ultra Violet (UV) Spectra Scanning of TEM

TEM was dissolved in ACN to a concentration of 0.05 mg/mL for injection, and the TEM was scanned for maximum absorption wavelengths in the range of 200–400 nm using a High Performance Liquid Chromatography (HPLC) diode-array detector (DAD).

Determination of TEM by HPLC

Establishment of HPLC conditions and linear equations for TEM. 1260 hPLC (Agilent, USA) was used; column: SEPAX C18, 4.6*250 mm, 5 μm, 120 Å; chromatographic conditions: mobile phase: ACN: water = 70: 30; flow rate: 1 mL/min; column temperature: 60°C; injection volume: 20 μL; detector: DAD; detection wavelength: 278 nm. TEM (25.0 mg) dissolves with ACN, dilute to 25 mL, formulates the solution of TEM with the concentration of 1 mg/mL, and then dilute to 0.001 mg/mL, 0.005 mg/mL, 0.01 mg/mL, 0.05 mg/mL, 0.1 mg/mL, 0.2 mg/mL, 0.25 mg/mL, 0.4 mg/mL, respectively. The limit of detection (LOD) and limit of quantification (LOQ) were set, and 0.001 mg/mL sample was used as the solution, and diluted to obtain 0.0001 mg/mL, 0.00003 mg/mL. 3 injections were made for each concentration, and the corresponding peak areas were recorded.

Evaluation of System Suitability and Precision

The TEM solution at a concentration of 0.05 mg/mL was taken and injected six times in parallel, and the peak area and peak-out time were recorded, respectively. The general acceptance criteria were separation (R) greater than 1.5, symmetry factor within the range of 0.85–1.15, relative to the average deviation of less than 2, and the number of plates (N) greater than 5000. The 0.5 mg/mL TEM master batch was prepared using ACN as solvent. 1 mL was pipetted into a 10 mL volumetric flask and titrated with ACN to the scale. Two experimenters diluted 6 samples in parallel in the same way and recorded the peak area and peak time.

Evaluate the Durability of the Method

The detection wavelength was varied ±2 nm from the original detection wavelength of 278 nm, that is, 280 nm and 276 nm. The flow rate was varied ±0.1 mL/min from the original flow rate of 1.0 mL/min, which was 0.9 mL/min and 1.1 mL/min. The mobile phase was varied between ACN: water = 68: 32–72: 28. The column temperature was varied ±2°C from the original column temperature of 60°C, ie, 58°C and 62°C.

Synthesis of mPEG-PBAE Diblock Copolymers and Preparation of pH-Responsive TEM-Loaded Micelles

Design and Preparation of mPEG-PBAE

The preparation process of mPEG-PBAE comprised three steps. First, solution A is obtained by ultrasonic dissolution of 10 g of poly(ethylene glycol) monomethyl ether 2000, 3 mL of triethylamine and 50 mL of methylene chloride; solution B is obtained by completely dissolving 1.2 mL of acrylamide in 25 mL of methylene chloride; and solution B is slowly added to solution A dropwise at 0°C, which lasts for 3 h and then refluxes at 40°C for 24 h. The organic phase is concentrated and 200 mL of cold n-hexane (−18°C) is added to the vacuum filtration and refining negative pressure drying to obtain mPEGA. The reaction equation is shown in Figure 1.

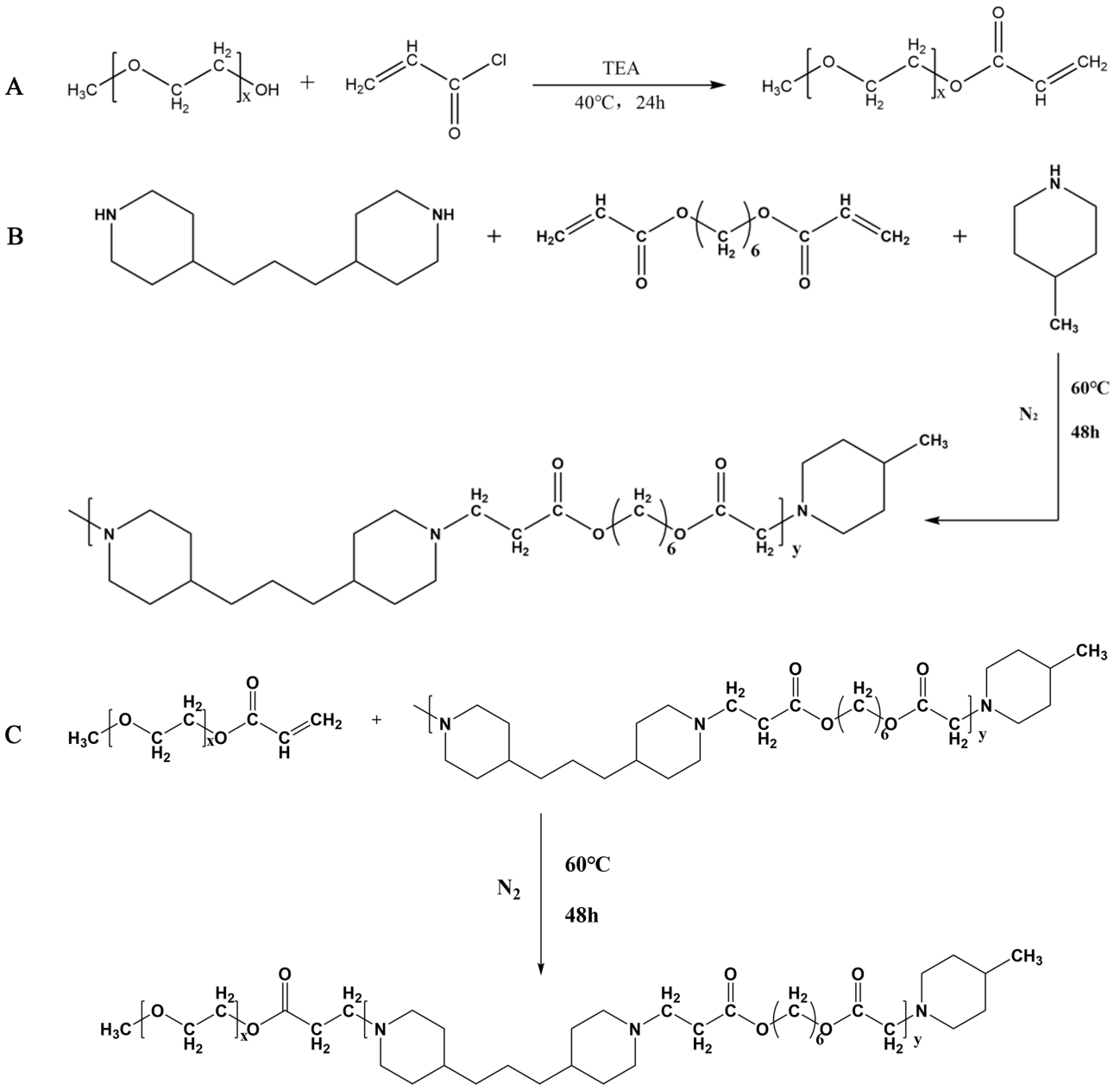

Figure 1 Synthesis route of pH-responsive mPEG-PBAE block copolymers. (**A**) Schematic illustration of synthesis for mPEGA. (**B**) Schematic illustration of synthesis for PBAE. (**C**) Polymerization of mPEG-PBAE block copolymer.

Abbreviations: TEA, triethylamine; mPEGA, methoxy poly(ethylene glycol) monoacrylate; PBAE, poly(beta-amino ester); mPEG-PBAE, poly(ethylene glycol) monomethyl ether-poly(beta-amino ester).

Then, 3 mmol 4-methylpiperidine, 9.9 mmol 1,3-bis(4-piperidyl)propane, 9 mmol 1,6-HDDA and 15 mL chloroform were reacted in an oil bath at 60°C in a nitrogen atmosphere for 48 h, and the concentrated reaction solution was heated and refined with −18°C cold ether and dried under negative pressure for 24 h to obtain PBAE. The reaction equation is shown in Figure 1.

mPEG-PBAE was synthesised by weighing 1:1 mPEG and PBAE and adding 25 mL of trichloromethane (TCM). The reaction in an oil bath at 60°C under nitrogen atmospheres for 48 h. The concentrated reaction solution was heated, the purification process was repeated three times, and the mPEG-PBEA was dried under negative pressure for 24 h. mPEG-PBEA copolymers with different ratios were gained according to the ratio of the input PBAE. The reaction equation is shown in Figure 1.

Examination of pH-Responsive Range and Critical Micelle Concentration (CMC)

50 mg of mPEG-PBAE was dissolved in 50 mL of deionized water, and the pH was adjusted to 3.0 with 0.1 mol/L HCL. 0.1 mol/L NaOH was titrated and the pH change was recorded.

CMC is a concentration above which an amphiphilic copolymer could form core-shell structured micelles. The CMC values of mPEG-PBAE in deionized water were estimated by using a standard pyrene fluorescence procedure. Pyrene, as a widely used fluorescence probe, is commonly used for the study of micelle formation and determination of CMC.[44–49] The mPEG-PBAE was prepared into aqueous solutions with concentrations of 0.5 mg/mL, 0.25 mg/mL, 0.1 mg/mL, 0.05 mg/mL, 0.025 mg/mL, 0.005 mg/mL, 0.001 mg/mL, 0.00025 mg/mL, and 0.00005 mg/mL, respectively. Pyrene solution of MeOH was transferred into glass bottles and the solvent was allowed to evaporate under mild heating. Polymer solutions with different concentrations were then added to the glass bottles. The final pyrene concentration was kept constant at 6×10^{-7} mol/L. The solutions were allowed to stand for 12 h at room temperature to achieve equilibrium. Fluorescence spectra were recorded by a spectrofluorometer. Emission wavelength was set at 390 nm and the micellization of mPEG-PBAE block copolymers was characterized by employing the excitation intensity ratio of third peak to the first peak (I_3 /I_1).[50] Upon formation of micelles, pyrene would move into the inside of the micelles from the aqueous phase, resulting in an alteration in the intensity ratio. The I_3 /I_1 value was then plotted vs the logarithm of polymer concentration. The CMC value was taken from the intersection of a fitted line of the curve at low polymer concentration (flat region) with a fitted line on a rapidly rising part of the curve. The CMC was assumed where a steep increase in fluorescence intensity was observed.[51,52]

Preparation of TEM-Loaded Micelles and Formulation Optimisation

The effects of hydrophobic segments and drug-carrier input ratio on encapsulation efficiency (EE) were studied. The mPEG-PBAE with hydrophobic chain segment polymerisation degree of 3, 5 and 7 were weighed, respectively, and the TEM input ranged from 10 to 50 mg. The EE was used as an investigation index, and the results were measured and recorded. mPEG-PBEA 175 mg, TEM 25 mg, and 10 mL of anhydrous MeOH was added and filtered by 0.22 μm nylon membrane, and then rotated and evaporated at 45°C for 15 min until the organic solvent was completely removed. Add 10 mL of deionised water at 45°C and fully hydrate at 180 rpm/min for 5 min in a constant temperature shaker. TEM-loaded micelles were obtained after filtration by 0.22 μm polyethersulfone membrane.

Determination of DLS and Zeta Potential

A Nanobrook 90Plus Zeta type potential and particle size analyser was used for the potential and particle size determination of TEM-loaded nanomicelles. Dynamic light scattering (DLS) and electrophoretic light scattering, were used to measure the electrophoretic mobility and Zeta potential of the particles, respectively. The 0.22 μm polyethersulfone membrane-filtered solution of TEM-loaded nanocolloids was diluted to 1 mg/mL with deionised water. Approximately 3 mL of the test solution was placed in a laser particle size analyzer for particle size and Zeta potential determination.

Morphological Characterization of TEM-Loaded Micelles

The prepared TEM-loaded micelles were added dropwise onto a 200 mesh copper grid covered with a carbon support film. The excess liquid was removed by filter paper and dried naturally at room temperature, and then put into the HT770 transmission electron microscope. The morphology was observed and photographed under 200 kV accelerating voltage.

Determination of Drug Loading Efficiency of TEM-Loaded Micelles

The concentration of TEM-loaded micelles solution was diluted to 1 mg/mL and ultracentrifuged at 10000 rpm/10 min. 0.5 mL of micelle solution before and after centrifugation was diluted and fixed to 10 mL with mobile phase. The TEM content in the samples was determined by HPLC-DAD method and the peak area was recorded.

Determination of Organic Solvent Residues in pH-Responsive TEM Nanomicelles Solutions

The gas chromatography (GC) method was used to determine 0.3% MeOH and pH-responsive TEM nanocellular solution with 0.3% MeOH residue as the limit. Injection volume: 1 μL; gasification chamber temperature: 250°C; column flow rate: 1.5 mL/min; split ratio: 1/10; column: DB-624 (30 mm×0.32 mm×1.8 μm); detector: flame ionization detector (FID); detector

temperature: 260°C; carrier gas: N_2; column temperature: column temperature 50°C (8 min) → 20°C/min → 250°C and hold (2 min).

Examination of the In vitro Release Properties of pH-Responsive TEM-Loaded Micelles

The in vitro release properties of TEM-loaded micelles were determined by dialysis method. 0.2 mL of 1 mg/mL TEM-loaded micelles was added into a dialysis bag (MWCO: 2000), and then the bag was placed into a beaker containing 99.8 mL of PBS (containing 0.5% Tween-80, pH 6.7 and 7.4, respectively), which was then placed into a 37°C 60 rpm/min constant-temperature shaker and shaken for a continuous period of time. 0.5 mL of release medium was taken out at 0.5, 1, 2, 4, 6, 8, 12, 24, and 36 h, and replenished with an equal volume of release medium at 37°C, respectively. The extracted samples were diluted and the TEM content was determined by HPLC. The cumulative release concentration was calculated and the in vitro release curve was plotted.

Pharmacodynamics and Safety Evaluation of TEM Nanomicelles

Haemolytic Experiments of TEM Nanomicelles

Erythrocytes collected from mouse blood were used to assess the haemolytic properties of mPEG-PBAE. Trilatone X-100 and saline were used as positive and negative controls. The mPEG-PBAE diblock copolymer was set at 25, 50, and 100 μg/mL (n = 3), respectively. The mouse orbital blood sampling was collected and diluted using 0.9% sodium chloride injection. The solution was transferred to a centrifuge tube and centrifuged at 2500 rpm for 15 min at 4°C to separate the blood cells, and the supernatant was carefully aspirated and discarded. The blood cells were diluted to 2% (v/v) by adding 0.9% sodium chloride injection to the separated blood cells. To the blood cells, 25, 50, and 100 μg/mL mPEG-PBAE solution were added, and 1% Trillatone X-100 solution and saline were added as positive and negative controls, respectively. All samples were incubated in a water bath at 37°C for 2 h and centrifuged at 2500 rpm for 15 min at 4°C. 100 μL of the supernatant was added to a 96-well plate, and the absorbance of the samples was detected using an enzyme marker at 540 nm. The formula for calculating the haemolysis rate is shown in eq 1:

$$\text{haemolysis rate} = \frac{A_{\text{sample}} - A_{\text{negative control}}}{A_{\text{positive control}} - A_{\text{negative control}}} \quad (1)$$

Cell Uptake Assay

Human renal clear cell adenocarcinoma cells 786-O were added to RPMI-1640 complete medium containing 10% FBS and 1% P/S, and cultured in an incubator at 37°C with 95% air and 5% CO_2. When the cells grew to about 90%, the medium was aspirated from the culture flask. Add PBS to the culture flask to wash the cells at the bottom of the flask and discard the PBS, and repeat the operation 2 times. After digestion with 0.25% trypsin/EDTA solution, RPMI-1640 complete medium was added to terminate the digestion. The cells were inoculated into six-well plates at a density of 6.5×10^5 cells/well, and continued to be cultured for 24 h. Weigh 20 mg of coumarin-6 and add 2 mL of DMSO to fully dissolve it, and then pipette 10 μL of the solution into 10 mL of the complete culture medium, which was the free drug solution. Since TEM does not have a fluorophore, coumarin-6 was selected as the model drug, the mPEG-PBAE TEM-loaded micelles of coumarin-6 were prepared according to the above method and diluted to the same drug concentration as that of the free drug group by adding to the complete culture medium, ie, the drug-loaded micelles solution. The cells were washed well with PBS, and 2 mL each of RPMI-1640 complete medium, free drug solution and drug-loaded micelles solution were added to the six-well plate. The cells were put into 37°C, 5% CO_2 incubator for further culture, and grouped into control group, free TEM group and TEM-loaded micelles group. After the cells were cultured for 4 h, the medium was aspirated out of the six-well plate and the culture was washed well with low-temperature PBS until the fluorescent dye was completely removed, and then digested in order to isolate the cells. Cells were resuspended with 500 μL of cryopreserved PBS in each group, and cellular uptake rate was examined using flow cytometry. Cells were washed sufficiently with low-temperature PBS to remove the un-uptaken coumarin-6 from the medium after 8 h. Six-well plates were placed under a fluorescence microscope to observe the fluorescence intensity in the cells.

CCK-8 Assay

The CCK-8 was used to measure the viability of cells. The groups were control group, mPEG-PBAE group (20 μmol/L, 30 μmol/L), TEM group (20 μmol/L, 30 μmol/L) and TEM-loaded micelles group (20 μmol/L, 30 μmol/L), and each group was set up with 6 groups of replicate wells. Here, the 786-O cell suspension was seeded into a 96-well flat-bottomed plate. After incubating overnight at 37 °C with 5% CO_2 for 24 h and 48 h, 10 μL CCK-8 solution was added per plate, and cells were incubated again for 3 h. We then measured the absorbance at 450 nm using a microplate reader at 24 h and 48 h, respectively, and the data were recorded and the cell survival rate was calculated. The calculation formula is shown in eq 2:

$$\text{Cell viability} = \frac{A_s - A_b}{A_c - A_b} \tag{2}$$

Evaluation of Anti-Tumour Therapeutic Effects in Mice

Logarithmically grown 786-O cells were isolated and made into cell suspension with PBS (pH=7.4) for cryopreservation. BALB/c-nude mice (6–8 weeks old, 18–20 g) were obtained from Fujian Wu's Experimental Animal Co., Ltd. (Fuzhou, China). All animal experiments were approved by the Experimental Animal Welfare and Ethics Committee of Fujian Provincial Hospital (IACUC-FPH-SL-20240220[0056]) and were conducted in accordance with the Law of the People's Republic of China on the Use of Laboratory Animals. Male BALB/c-nude mice (6–8 weeks) that were acclimatised for 2 weeks were randomly divided into 4 groups (5 mice per group). Fix the back of the mice and inject the cell suspension subcutaneously in the axilla using an insulin injection needle (flick the EP tube to mix the cells well before injection), with 1×10^6 cells per mouse. Control group: normal saline (NS). Blank micelles group: weigh mPEG-PBAE 175 mg precisely and prepare blank micelles by film hydration method, which was added to 5 mL deionised water for complete hydration. Free TEM group: Appropriate amount of TEM was weighed and anhydrous ethanol was used to configure the TEM solution with a concentration of 50 mg/mL. Then add water for injection containing 5% Tween 80% and 5% polyethylene glycol 400, and dilute the concentration of TEM to 2.5 mg/mL. TEM-loaded micelles group: weigh mPEG-PBAE 175 mg and TEM 25 mg, and prepare TEM-loaded micelles by thin-film hydration method, which were fully hydrated by adding 5 mL of deionized water.

Each mouse was administered according to the effective concentration of TEM 20 mg/kg, and the blank micelle group was administered an equivalent carrier dose converted according to the drug-carrying capacity of TEM nanomicelles. Every 3 days since the ectopic termination tumour model construction was completed, the length and width of the tumours were measured using vernier calipers and the tumour volume was calculated (V = length × width/2). Mice in each group were executed after the 30th day of tumour growth, and the subcutaneous tumours were dissected out, measured and photographed.

Hepatotoxicity and Nephrotoxicity Experiments in Mice

Male BALB/c-nude mice were acclimatised for 2 weeks and then randomly divided into 4 groups (5 mice per group). Blood was collected retroorbitally from mice in each group 24 h after drug administration, and serum was separated from the collected blood. Alanine aminotransferase (ALT), aspartate aminotransferase (AST), creatinine (Cr) and blood urea nitrogen (BUN) were measured according to the instructions of the kit.

Results

Establishment and Evaluation of HPLC Methodology for TEM

The maximum absorption wavelength of TEM was 278 nm, so this wavelength was selected as the detection wavelength of TEM (Figure 2A). The elution peak time of TEM was 10.562 min, the symmetry factor was 0.96, and the number of plates was 7106 (Figure 2B). Supplementary Table 1 shows that the regression line equation as well as the correlation coefficient were y = 45961x+44.806 and R^2= 0.9995, respectively. The results showed that the TEM peak area was linearly related to the concentration in the concentration range of 0.001 to 0.4 mg/mL (Figure 2C).

The acceptance criterion for the detection limit was a signal-to-noise ratio of not less than 3 (Supplementary Table 2), and the acceptance criterion for the quantification limit was a signal-to-noise ratio of not less than 10 (Supplementary

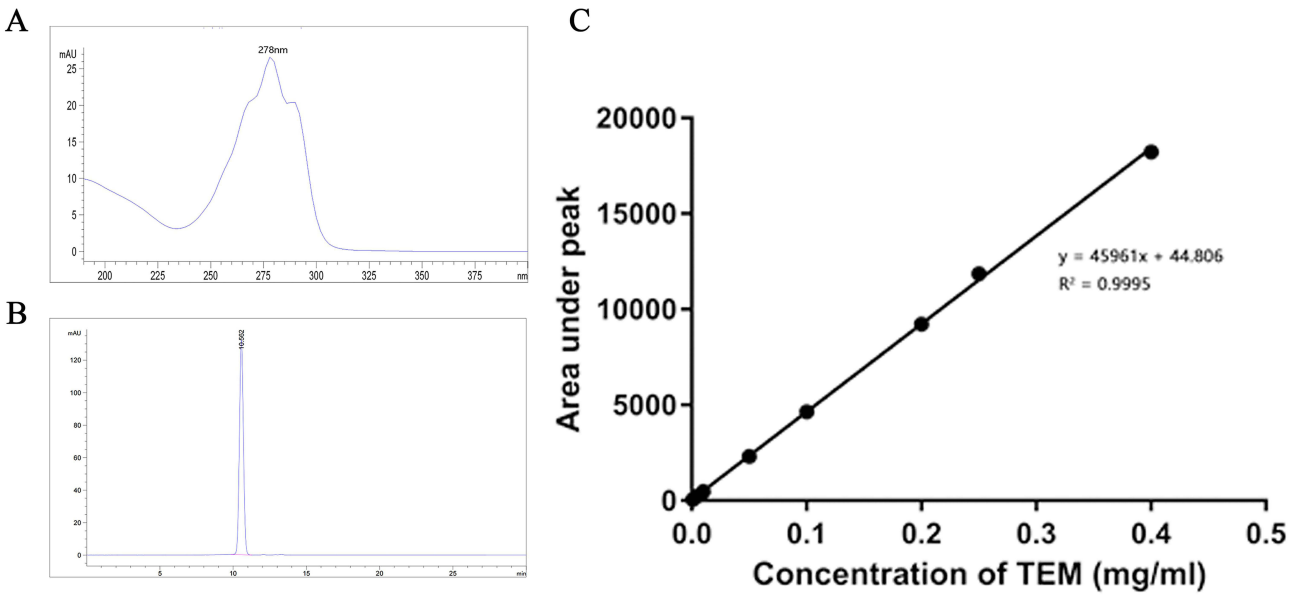

Figure 2 Establishment and evaluation of HPLC methodology for TEM. (**A**) UV full-wavelength scanning chromatogram. (**B**) HPLC spectrum of TEM. (**C**) Standard curve of TEM.
Abbreviations: HPLC, high performance liquid chromatography; TEM, temsirolimus; UV, ultra violet.

Table 3). The TEM solution at a concentration of 0.05 mg/mL was taken and injected six times in parallel, and the peak area and peak-out time were recorded, respectively. The general acceptance criteria were separation (R) greater than 1.5, symmetry factor within the range of 0.85–1.15, deviation relative to the mean less than 2, and number of plates (N) greater than 5000 (Supplementary Table 4). As shown in Supplementary Table 5, there was a small deviation in the assay results from different experimenters, and the precision of the HPLC method was good. The durability of the method was examined when there were small fluctuations in the test conditions (Supplementary Table 6).

TEM has good linearity in the concentration range of 0.001–0.4 mg/mL concentration, and the method has good linearity, LOD, LOQ, system applicability and precision, but the method durability needs to be further optimized. The method was only applied to the determination of EE and in vitro release rate for this preparation.

Synthesis of mPEG-PBAE Diblock Copolymer and Preparation of pH-Responsive TEM-Loaded Micelles

The intermediate product mPEGA obtained from the synthesis was structurally characterized by ^{1}H NMR analysis. The reaction product was fully dried in a vacuum drying oven to remove water, and the dried mPEGA was dissolved in deuterated chloroform ($CDCl_3$) for ^{1}H NMR analysis. As shown in Figure 3, the three characteristic signals of hydrogen atoms in the double bond in the chemical structure of the product were at δ = 5.82 ppm, δ = 6.14 ppm, and δ = 6.41 ppm, respectively. mPEGA had a duplicate methylene embodiment at δ = 3.62 ppm, and the methoxy group was located at δ = 1.40 ppm. Figure 4 shows that mPEG at a concentration of 0.5 mg/mL showed an absorption peak at 7.214 min, whereas mPEGA at a concentration of 10 mg/mL under the same liquid-phase conditions did not show an absorption peak at this time point. mPEG residue in the mPEGA product was less than 5%. Therefore, the residual mPEG could be completely removed according to this preparation and refinement method. mPEG-PBAE, which was fully dried, was dissolved in $CDCl_3$, and the results of the ^{1}H NMR analysis are shown in Figure 5. The characteristic peak of poly (ethylene glycol) monomethyl ether repeating unit was at δ=3.61 ppm. The three characteristic hydrogens of the piperidine group were at δ=2.59 ppm, δ=2.76 ppm, and δ=2.96 ppm. The two characteristic signals of the methylene hydrogen at the hydrophobic end near the ester group were at δ=4.04 ppm. Based on the above data, the successful synthesis of pH-responsive amphiphilic block copolymer mPEG-PBAE was confirmed.

The amine group of the piperidine moiety in the hydrophobic segment undergoes binding with protons in an acidic environment and releases the bound H^{+} with the increase of pH, thus the pH-responsive amphiphilic block copolymer

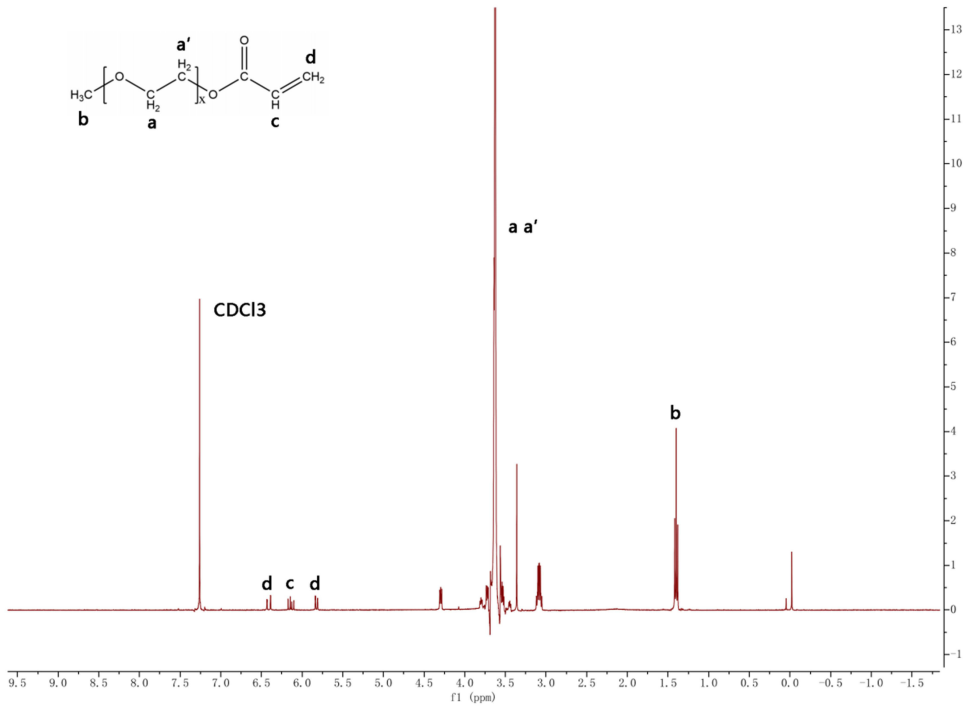

Figure 3 The ^{1}H NMR spectrum of mPEGA.
Abbreviations: mPEGA, methoxy poly(ethylene glycol) monoacrylate; NMR, nuclear magnetic resonance.

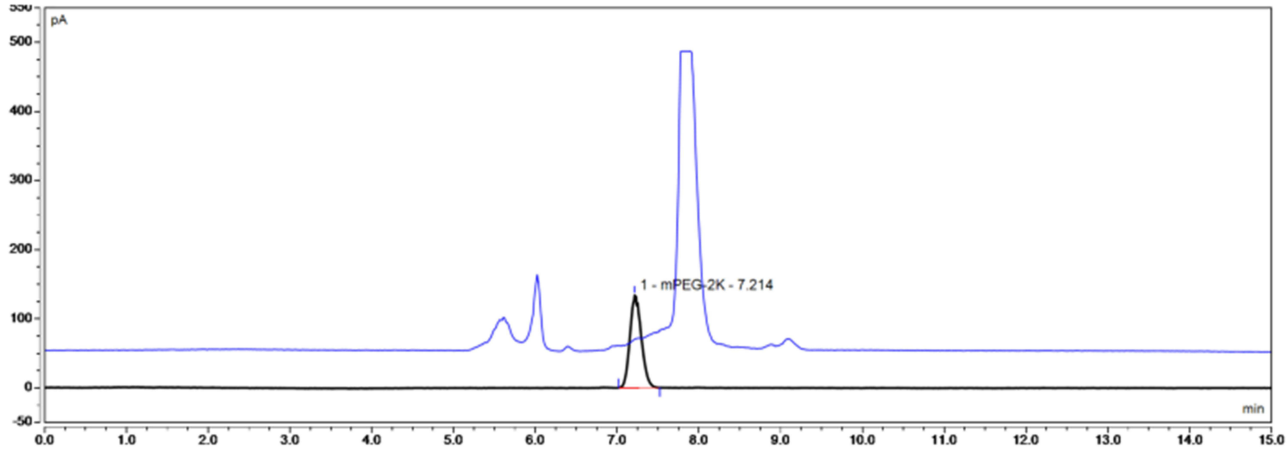

Figure 4 HPLC-CAD patterns: (black) 0.5 mg/mL mPEG; (blue) 10 mg/mL mPEGA.
Abbreviations: HPLC-CAD, high performance liquid chromatography-charged aerosol detector; mPEGA, methoxy poly(ethylene glycol) monoacrylate; mPEG, methoxy poly(ethylene glycol).

shows buffering effect in the pH range of 6.5 to 7.5 (Figure 6). When the concentration of block copolymers exceeds their CMC, the block copolymers can self-assemble into micelles in aqueous solution. The formation of micelles from the block copolymers is verified by the fluorescence probe technique using pyrene. The fluorescence emission spectrum of pyrene probe can reflect the fine variation of the vibrational energy level of the ground state. The fluorescent intensity ratio of the third peak (I_3, 333 nm) to the first peak (I_1, 339 nm) (I_3/I_1) is strongly dependent on the environmental polarity of pyrene. In block copolymer solution, pyrene can be solubilized into micelles when the concentration of block copolymers exceeds CMC. As a result, the polarities of pyrene solutions before and after the micelle formation are greatly different. Therefore, the sharp increase in I_3/I_1 value confirms the successful formation of mPEG-PBAE micelles. The corresponding critical concentration value (0.036 mg/mL) is the CMC of mPEG-PBAE block copolymers (Figure 7).

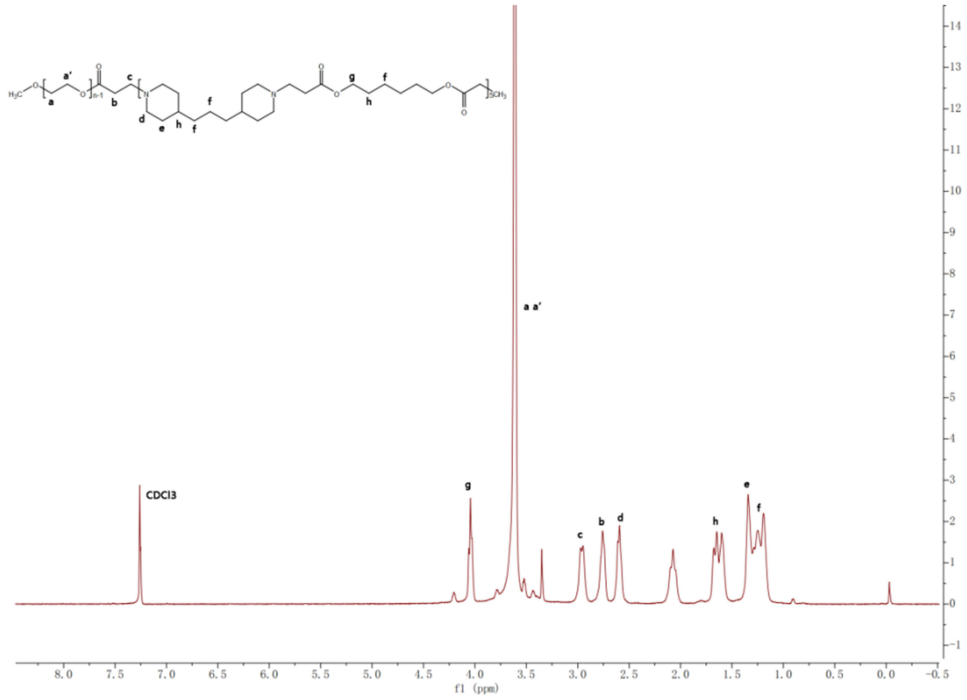

Figure 5 The ^{1}H NMR spectrum of mPEG-PBAE.
Abbreviations: NMR, nuclear magnetic resonance spectroscopy; mPEG-PBAE, poly(ethylene glycol) monomethyl ether-poly(beta-amino ester).

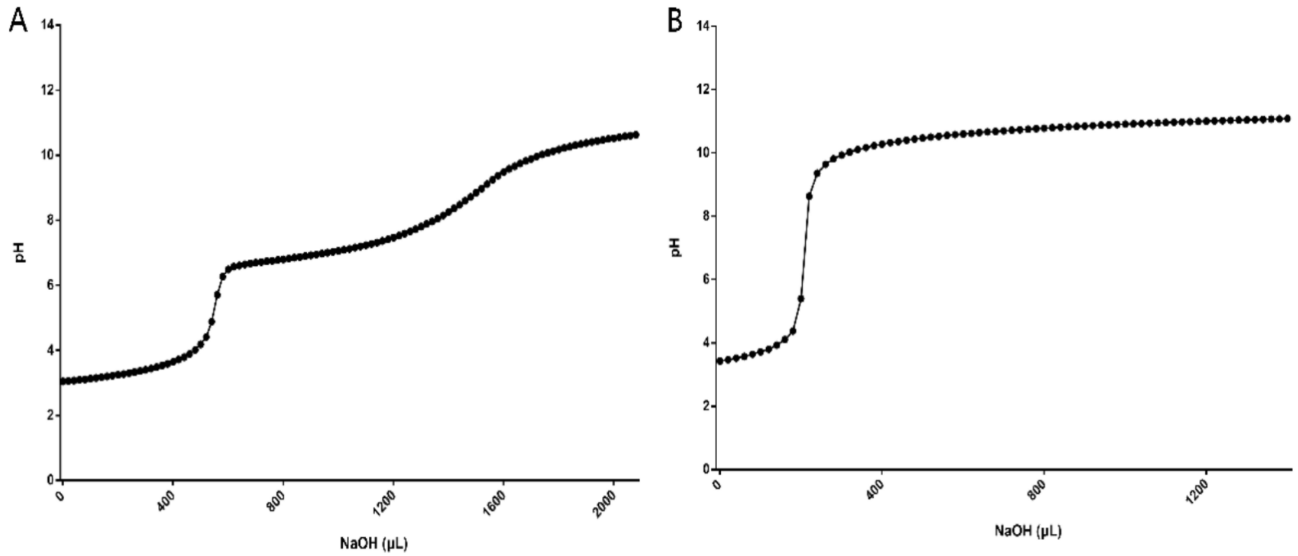

Figure 6 pH-responsive titration curves of (**A**) mPEG-PBAE; (**B**) piperidine.
Abbreviation: mPEG-PBAE, poly(ethylene glycol) monomethyl ether-poly(beta-amino ester).

Excessive carriers into the body will burden the metabolic system and pose a biosafety risk, and thus the amount of pharmaceutical excipients should be reduced as much as possible while achieving targeted drug delivery. Fixing the dosage of mPEG-PBAE at 175 mg, the increase of TEM input will lead to the decrease of EE. When the length of the hydrophilic chain segments of the diblock copolymer was frozen, the EE of the TEM-loaded micelles increased with the rise in the polymerization of the hydrophobic chain segments, which could be explained by the fact that the greater diameter of the hydrophobic core allowed more fat-soluble drugs to be loaded. Since the polymerization degree of mPEG-PBAE hydrophobic chain segments had a direct effect on the pH response range and particle size, the optimal

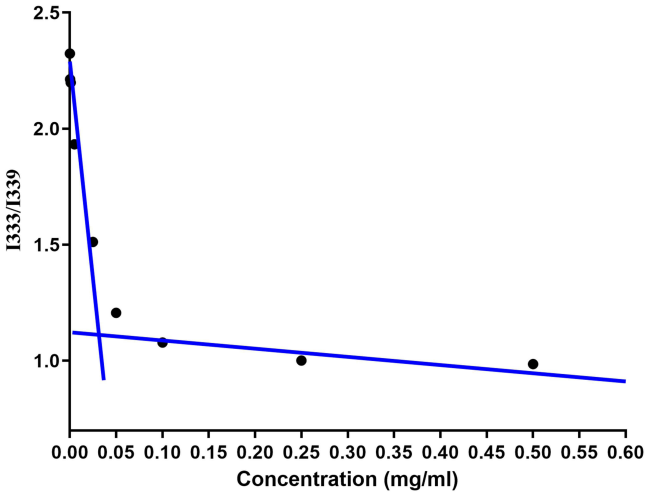

Figure 7 CMC results of mPEG-PBAE diblock copolymer.
Abbreviations: CMC, critical micelle concentration; mPEG-PBAE, poly(ethylene glycol) monomethyl ether-poly(beta-amino ester).

prescription was selected from the response values corresponding to each factor combined: mPEG: PEAB = 1: 5; TEM input: 25 mg; mPEG-PBAE input: 175 mg (Figure 8).

The particle size distribution was determined by DLS method, which showed that the average particle size of the pH-responsive TEM nanoclusters was 43.83 nm. The polydispersity indexes (PDI) of drug-loaded micelles (determined by DLS using a variant of the so-called cumulants method)[53] are 0.05, indicating uniform micelle sizes, and the NPs analysed by TEM are monodispersed. The Zeta potential of the micelles was 1.79 mV by electrophoretic light scattering (Figure 9). The sizes of dried micelles observed by TEM, are slightly smaller than their hydrodynamic diameters measured by DLS. From transmission electron microscopy, mPEG-PBAE and TEM formed spherical or spheroidal nano-ions in water according to the principle of similar phase solubility under the action of surface tension, with a particle size of about 50 nm and a more homogeneous size distribution. The morphology observed under transmission electron microscopy showed consistency with the results of particle size determination (Figure 10).

In this experiment, the EE of pH-responsive nanocolloids with 12.5% TEM loading was investigated, and the EE of nanocolloids was calculated to be 95.27%. This shows that the prepared pH-responsive amphiphilic block copolymers have a good match with TEM (Supplementary Table 7). The solubility of TEM in water was significantly increased from 2.6 μg/mL to over 5 mg/mL.

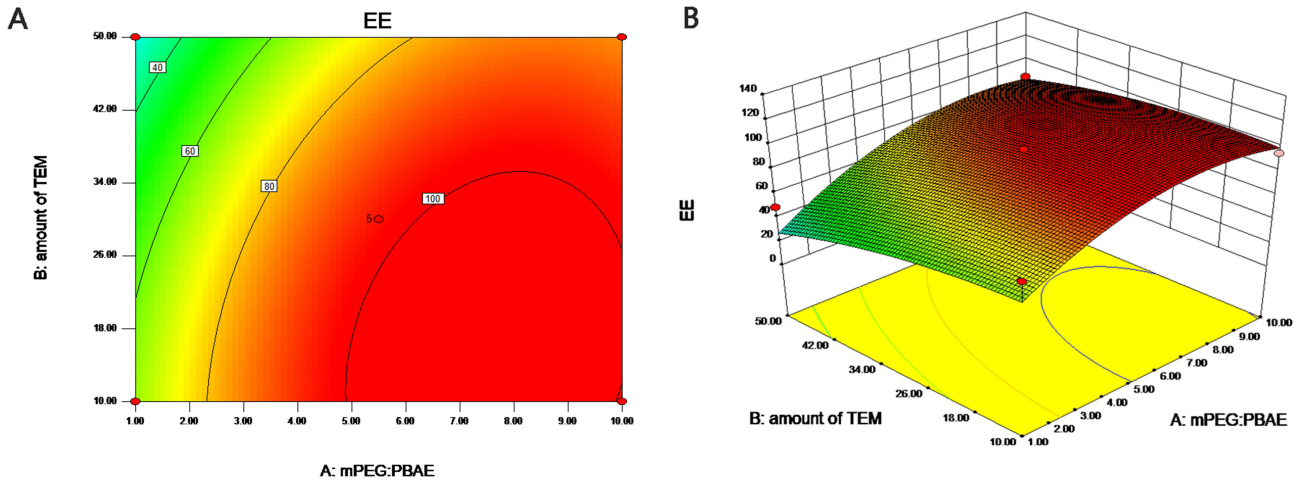

Figure 8 Prediction of correlation factors affecting encapsulation rate. (**A**) 2D contours; (**B**) 3D response surface modeling.
Abbreviations: mPEG-PBAE, poly(ethylene glycol) monomethyl ether-poly(beta-amino ester); TEM, temsirolimus.

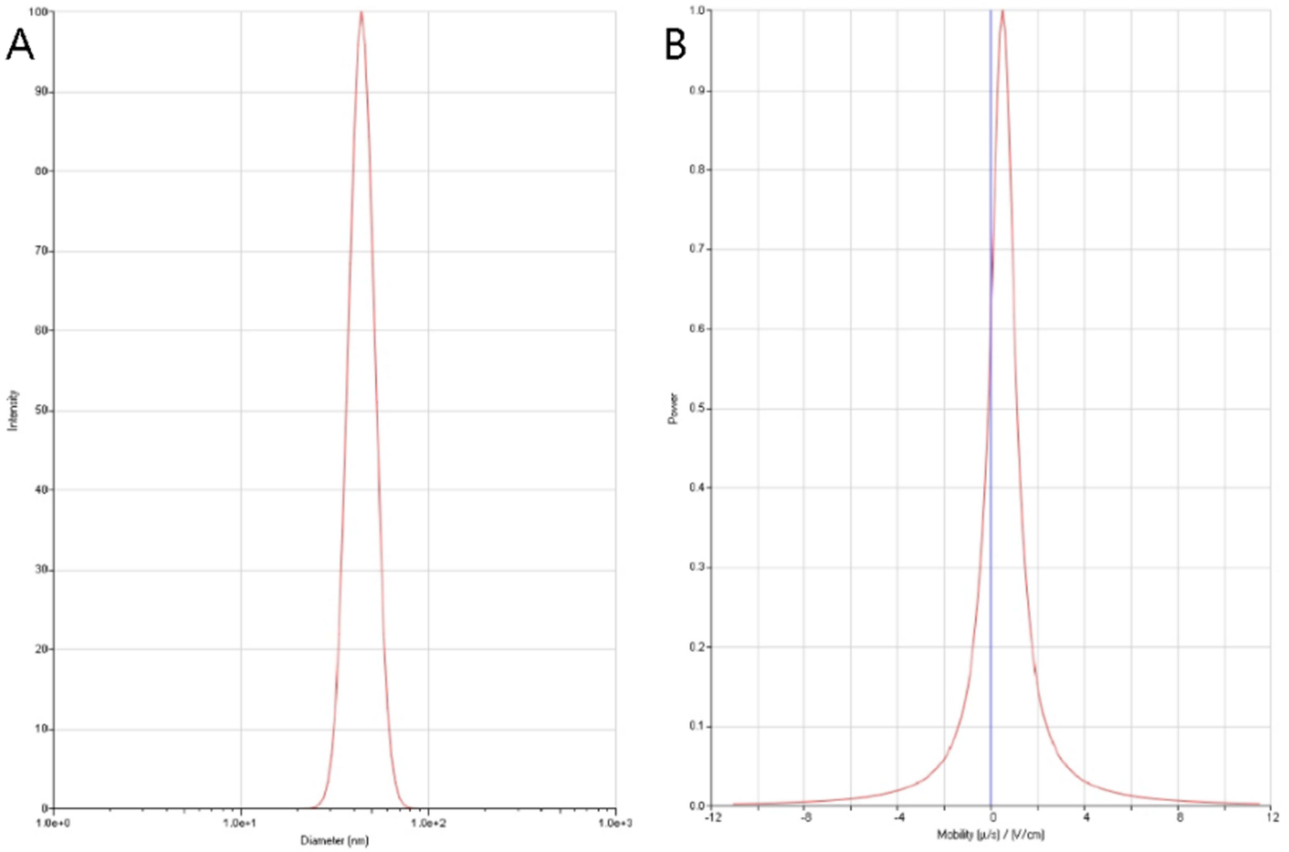

Figure 9 Characterization of pH-responsive TEM-loaded micelles. (**A**) particle size and distribution; (**B**) Zeta potential.
Abbreviation: TEM, temsirolimus.

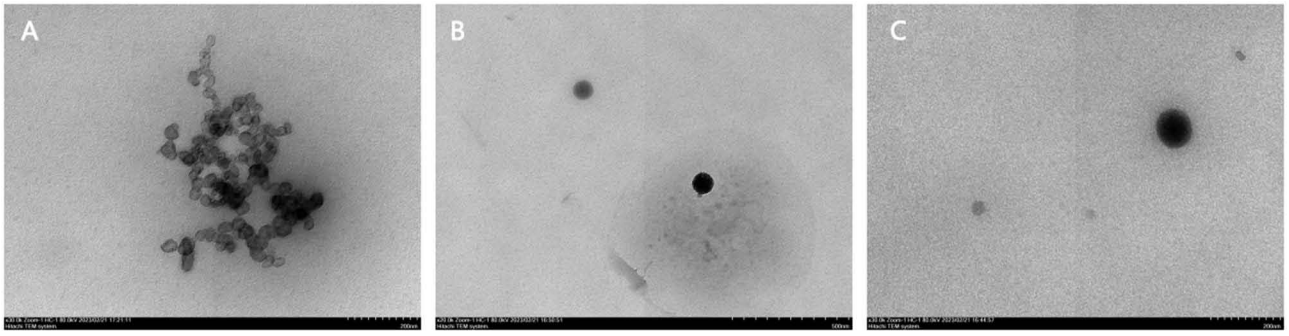

Figure 10 Transmission electron micrograph of pH-responsive TEM-loaded micelles. (**A**), (**B**), and (**C**) show transmission electron micrographs of pH-responsive TEM-loaded micelles at different magnifications.
Abbreviation: TEM, temsirolimus.

The GC method was used to determine the 0.3% MeOH and TEM-loaded micellar solutions, respectively. As shown in Figure 11, the MeOH peaked at 2.725 min, while the TEM-loaded micelles solution did not show absorption peaks at that time, so the pH-responsive TEM-loaded micelles prepared by thin-film hydration method can completely remove MeOH and have high safety. PBS at pH 7.4 and 6.7 was used to simulate the environment of human normal and tumor tissues, respectively, to investigate the intelligent response performance of the drug-loaded micelles. Figure 12 shows that the TEM-loaded micelles had a stable carrier structure and slow drug release at pH 7.4, with only 29.94% of the total release measured at 36 h. In the simulated tumor environment, the TEM was released rapidly from 0 to 12 h, with

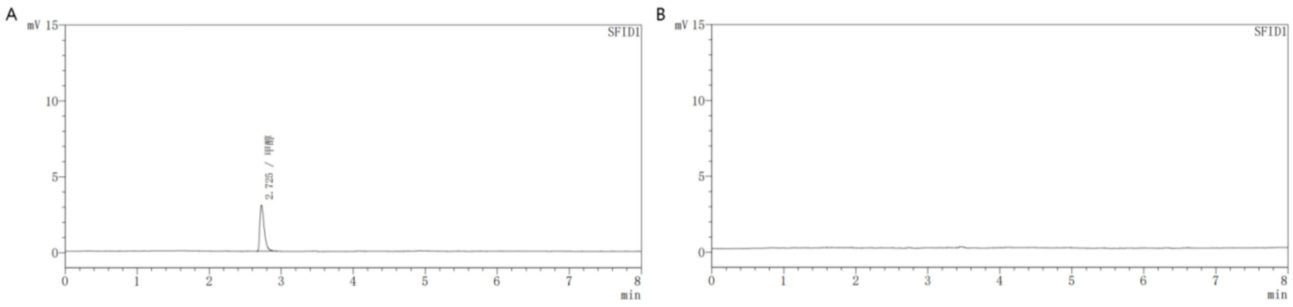

Figure 11 GC mapping of (**A**) 0.3% methanol; (**B**) pH-responsive TEM-loaded micelles.
Abbreviations: TEM, temsirolimus; GC, gas chromatography.

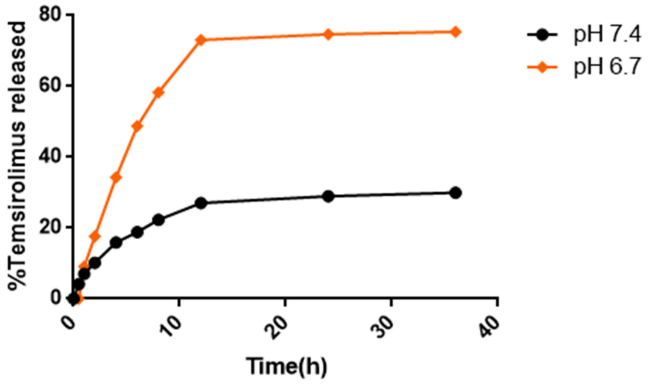

Figure 12 Release rates of pH-responsive TEM-loaded micelles at pH 6.7 and 7.4.
Abbreviation: TEM, temsirolimus.

a release rate of up to 73.12%. In summary, the release of TEM-loaded micelles had significant pH-dependent characteristics, and the in vitro release rate was consistent with the results of acid-base titration of the block copolymer.

In the thin film hydration method, also known as Bangham method, we choose MeOH as the solvent to fully dissolve the drug and carrier, and remove the organic solvent by rotary evaporation under vacuum, so that the drug and carrier can be fully mixed and form a homogeneous film. Then water was added, and the hydrophobic effect prompted the rapid aggregation of the hydrophobic ends of TEM and mPEG-PBAE diblock copolymer to form a uniform spherical structure by surface tension. The average particle size of the TEM-loaded nanoparticles was 43.83 nm, and PDI was 0.05, indicating that the micelles had good and homogeneous physicochemical properties. The in vitro release rate of the TEM-loaded micelles was examined, and the release rate of TEM had a significant pH dependence, which was consistent with the results of the pH response range determination of the mPEG-PBAE diblock copolymer, confirming that the TEM-loaded micelles had the unique property of pH sensitivity.

TEM Nanocolloid Pharmacodynamics and Safety Evaluation

To evaluate the in vivo safety of TEM-loaded micelles, a hemolysis test was performed. Compared with the Trilatone X-100 group, 25 and 50 μg/mL mPEG-PBAE did not produce significant hemolytic effects, so the preparation of TEM-loaded micelles using mPEG-PBAE had non-hemolytic properties (Figure 13A). mPEG-PBAE showed a small portion of hemolysis at a concentration of 100 μg/mL, which may be due to the shielding effect of the nanoparticle PEG shell on the internal positive charge. The results of flow cytometry and fluorescence microscopy showed that 786-O cells were inefficient in uptake of free coumarin, and mPEG-PBAE greatly increased the internalization of coumarin-6 by the cells by means of encapsulation (Figure 13B and C). Our results showed that mPEG-PBAE diblock copolymers significantly improved the efficiency of cellular internalization of drugs, which was attributed to the enhancement of lattice protein-mediated cellular uptake and niche protein-mediated endocytosis on the surface of tumor cells by TEM nanoparticles.[54]

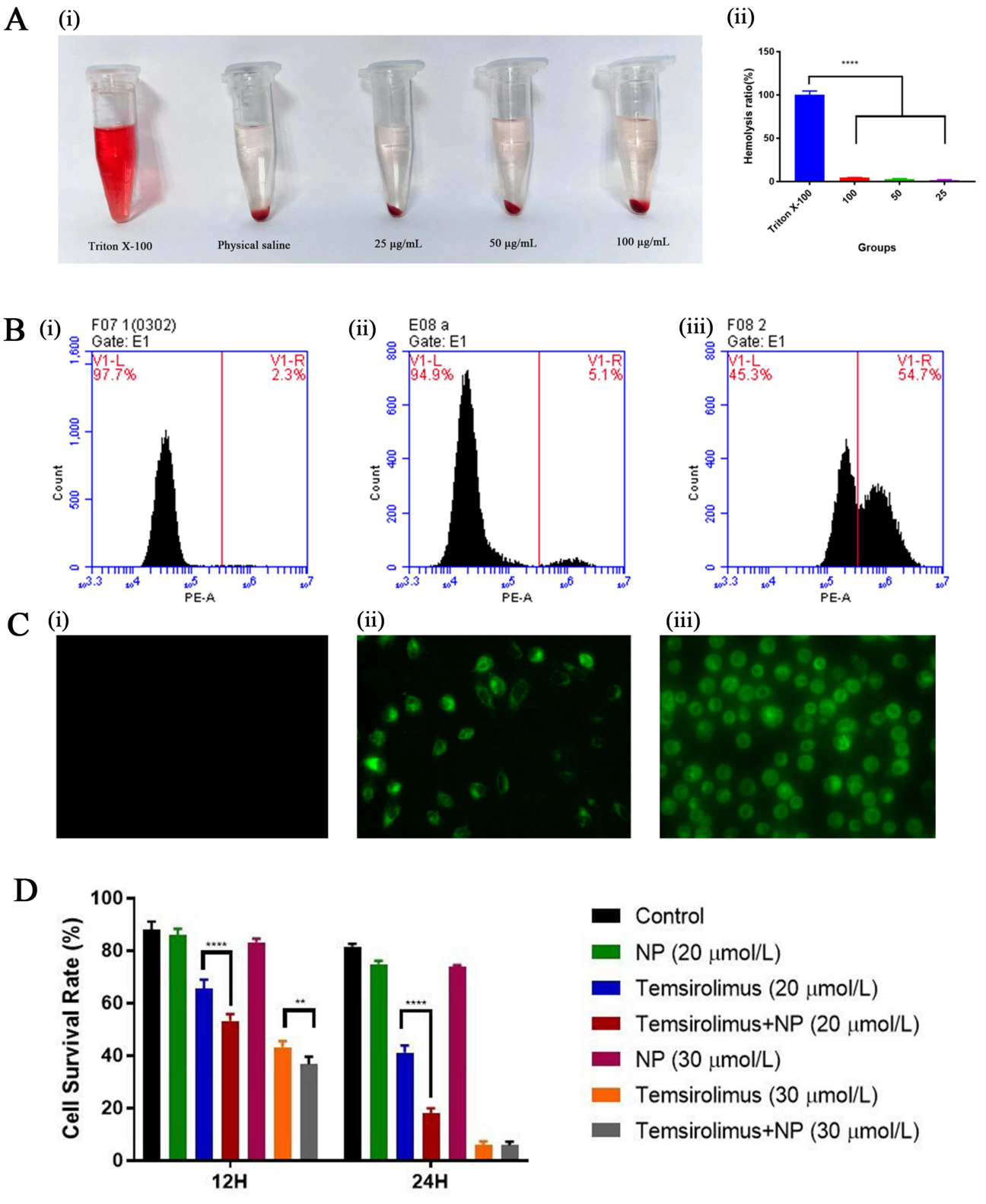

Figure 13 Continued.

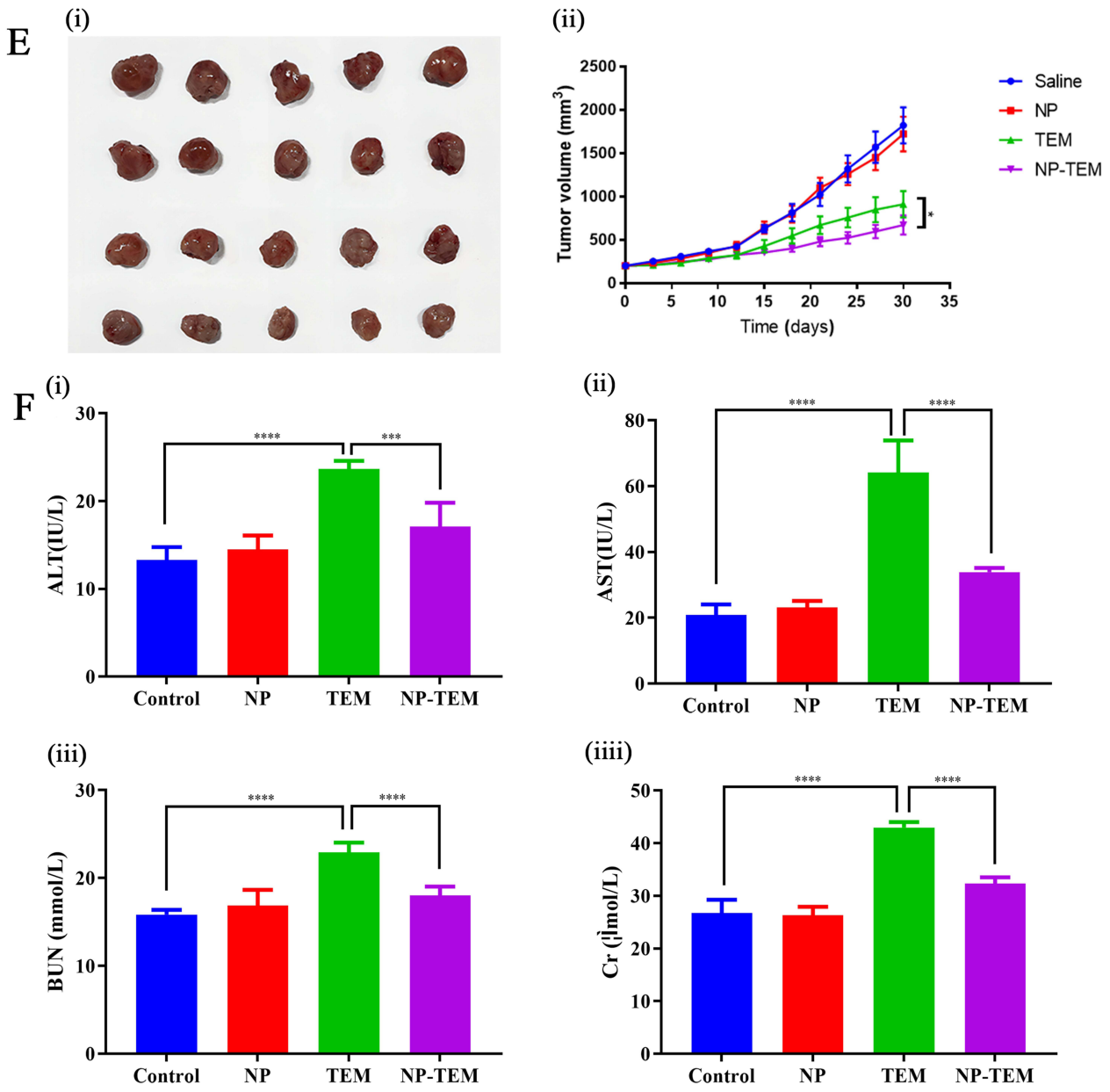

Figure 13 Antitumor effect of drug delivery system in vivo. (**A**) In vitro hemolysis assay of mPEG-PBAE (25~100μg/mL): (i) hemolysis experimental phenomenon; (ii) mPEG-PBAE concentration–hemolysis ratio. (**B**) Flow cytometry was performed to analyze cellular uptake of drug after 4 hours: (i) control group; (ii) free TEM group; (iii) TEM-loaded micelles group. (**C**) Fluorescence microscopy was performed to analyze cellular uptake of drug after 8 hours: (i) control group; (ii) free TEM group; (iii) TEM-loaded micelles group. (**D**) The effect of pH-responsive TEM-loaded micelles on the survival rate of 786-O cells. (**E**) Anticancer efficacy based on (i) tumor image; (ii) tumor volume. The number of mice in each group was 5, and the groups in (i) from top to bottom were normal saline group, NP group, TEM group and NP-TEM group. (**F**) The effect of pH-responsive TEM-loaded micelles on liver and kidney in mice based on (i) ALT; (ii) AST; (iii) BUN; (iiii) Cr. (*p<0.05; **p<0.01; ***p<0.005; ****p<0.001).
Abbreviations: TEM, temsirolimus; mPEG-PBAE, poly(ethylene glycol) monomethyl ether-poly(beta-amino ester); NP, nanoparticle; ALT, alanine aminotransferase; AST, aspartate transaminase; BUN, blood urea nitrogen; Cr, creatinine.

Comparison of the effects of blank micelles, free TEM, and TEM micelles at concentrations of 20 μmol/L and 30 μmol/L on the viability of 786-O cells at 12 h and 24 h (Figure 13D). At 12 h, the cell viability of both 20 μmol/L and 30 μmol/L TEM micelles groups was significantly lower than that of the free TEM group, and at 24 h, only the 20 μmol/L TEM micelles group showed significant differences. Therefore, only a small number of cells survived in both the free TEM group and the TEM micelle group, while no significant difference was noted between the 30 μmol/L TEM micelle group and the free TEM group. However, prolonged exposure to 30 μmol/L TEM intervention resulted in substantial

cytotoxicity, leading to only a small number of surviving cells in both the free TEM and TEM micelle groups. Additionally, compared to the control group, the blank micelle group did not exhibit significant inhibitory effects on the cells. Both TEM micelles and free TEM, at concentrations of 20 μmol/L and 30 μmol/L, demonstrated notable inhibitory effects on the cells compared to the control group, regardless of whether it was 12 h or 24 h after treatment.

Mice with axillary loaded tumors were randomly grouped and injected with NS, blank micelles, free TEM and TEM-loaded micelles via tail vein. Tumor growth was shown in Figure 13E. We found that the control mice, which administered NS and free micelles, exhibited rapid tumor growth, whereas tumor growth was slowed in response to TEM administration. Importantly, TEM-loaded micelles exhibited more significant tumor growth inhibition relative to free TEM. These findings clearly demonstrated the improved therapeutic efficacy of TEM-loaded polymeric micelles, as they improved TEM delivery to the tumors owing to the de-micellization that occurred only in acidic intracellular or intratumoral environments.

The biochemical parameters change in serum was related to nephrotoxicity and hepatotoxicity parameters in the experimental mice groups.[55] Under normal conditions, Cr and BUN could be filtered by glomerulus and excreted in the urine. Once renal failure occurs, the glomerular filtration function would decline, leading to the elevation of serum Cr and BUN.[56] The elevation of serum transaminases like ALT, AST is indicative of hepatocyte damage leading to increase in cell membrane permeability that facilitates transaminases leak out to bloodstream.[57] To further evaluate the biosafety of TEM-loaded micelles, saline, blank micelles, free TEM and TEM-loaded micelles were administered to healthy mice by tail vein injection, and the blood biochemical indices of mice were measured. ALT, AST, BUN and Cr detected in serum samples are standard parameters for evaluating liver and kidney function. As shown in Figure 13F, compared with the control group, the levels of blood biochemical indicators ALT, AST, BUN and Cr in mice after free TEM treatment were significantly increased, while the increasing trend of ALT, AST, BUN and Cr after treatment with TEM-loaded mPEG-PBAE micelles was significantly inhibited, indicating that mPEG-PBAE micelles can reduce the liver and kidney damage caused by TEM, and the material has reliable safety.

Discussion

In this study, we successfully prepared pH-responsive TEM-loaded mPEG-PBAE copolymer micelles. The nanodrug delivery system exhibited good water solubility, passive targeting and low toxicity in vivo, and its significant anti-tumor activity was observed.

Polymers, especially pH-responsive block copolymers, have been pursued by researchers because of their excellent delivery efficiency, predictable structure and characteristics of pH response.[58,59] The pH-stimulus PMs have been investigated and used as a main trigger for inducing drug release. It is well known that micro-environments of tumor cells show a relatively lower pH than normal tissues because of their high preference of glycolysis only at aerobic conditions, which leads to lactic acid accumulation.[60] The microacidic conditions of the tumor microenvironment are an important basis for achieving rapid release of antitumor drugs. mPEG-PBAE diblock copolymers were designed and synthesized, in which the tertiary amine groups of the piperidine moiety in the hydrophobic chain segments can be protonated to achieve the hydrophobic–hydrophilic transition under acidic conditions in order to disrupt the integrity of the nanoparticles for the release of the TEM. The difficulty in realizing this idea lies in the control of mPEG-PBAE's molecular weight so that its pH range matches that of the solid tumor microenvironment, that is, pH 6.5–7.4. We performed a systematic study, by synthesizing a series of mPEG-PBAE diblock copolymers with different ratios, it was found that the pH response of the material was in the range of 6.5–7.5 when the polymerization degree of the hydrophobic segment was 5.

TEM is used as a first-line drug for high-risk RCC patients, and one of the challenges in clinical practice is due to its hydrophobic physicochemical properties. TEM is a lipid-soluble drug, which can spontaneously form a hydrophobic core with amphiphilic block copolymers in aqueous solution according to the principle of similar dissolution, achieving the purpose of delivering TEM. By using amphiphilic block copolymers as drug delivery vehicles, the solubility of TEM in water can be greatly increased from 2.6 μg/mL to more than 5 mg/mL.

Nanodelivery is used for drug delivery, where drugs are packaged into nanoscale particles to be transported to target cells, thereby reducing damage to healthy cells and increasing the efficacy of the drug. To establish the clinical relevance of our

TEM-loaded nanomicelles, we investigated in vivo toxicity by measuring the levels of cell hemolysis, kidney, and liver markers. The liver and kidneys are the primary organs responsible for the metabolism and excretion of drugs and molecules, and if the liver and kidney cells are damaged, their markers will increase accordingly. The results showed that mPEG-PBAE diblock copolymers have lower hematological toxicity and hepatorenal toxicity, and the wrapping of TEM can also reduce the hepatorenal toxicity of the drug, which may be due to the stealthy properties of the PEG shell of the nanoparticles. PEG is classified as "Generally Recognized as Safe" (GRAS) by the US Food and Drug Administration (FDA) and has been used in the manufacture of nanoparticles. PEG is classified by the US FDA as a polymer that is GRAS. A large number of marketed drugs and a long history of clinical applications have confirmed the biocompatibility of PEG. The stealth properties of PEG stem from the molecular structure and physical characteristics. Firstly, PEG is extremely hydrophilic, with each glycol subunit surrounded by at least 2–3 water molecules.[61,62] As a result, the PEG shell produces a hydrated layer with a certain thickness and its spatial site resistance prevents biomolecules from penetrating into the polymer layer and binding to the drug in the core through hydrophobic or electrostatic interactions.[63–65] Secondly, PEG is highly flexible, which leads to a large amount of polymer chain conformations, so that biomolecules crossing the hydrophilic outer layer lead to a change in the PEG conformation, however the reduction in degrees of freedom is thermodynamically difficult.[10,11,66] In summary, these features greatly protect the interaction between the TEM and the biological environment.

Cell survival and tumor inhibition experiments confirmed the significant potentiation of mPEG-PBAE diblock copolymers for the efficacy of TEM. In addition to increasing the intracellularization of TEM by tumor cells, the passive targeting and pH-controlled release of the nanoparticles may also be the key factors for strengthening the effect of TEM. At a concentration of 20 μmol/L, TEM in conjunction with mPEG-PBAE exhibits heightened cytotoxicity towards tumor cells and tissues. This phenomenon can be attributed to the amphiphilic polymeric functionality of these micelles, which enhance membrane mobility and micelle diffusion into these tumor cells. After these micelles are taken into cells, they dissociate when exposed to acidic lysosomal conditions, thus allowing TEM to accumulate intracellularly. Additionally, polymer micelles may prevent drug efflux from P-glycoprotein (P-gp) pump by inhibiting P-gp expression, thus increasing the intracellular drug concentration and enhancing antitumor activity.[67,68] In contrast to the control group, both 30 μmol/L free TEM and TEM-loaded micelles demonstrated robust tumoricidal effects in a 24 h experiment, albeit without significant differentiation between the two groups. This might stem from the rapid release of TEM from the drug-loaded micelles within the first 12 h in simulated tumor environments, reaching a release rate of 73.12% beyond this point, insufficient for complete TEM release.

Interestingly, Cai Hua's research has developed a chimeric peptide-engineered nanomedicine (designated as PRS) for the synergistic suppression of tumor growth in an orthotopic breast cancer model. Within this nanomedicine, the tumor matrix-targeting peptide palmitic-K (palmitic) CREKA can self-assemble into a nano-micelle to encapsulate Rapamycin (mTOR inhibitor).[69] However, this study lacks an assessment of the water solubility of the nanomicelles, and the effect on RCC models remains unknown. Yu Tong Tam prepared an oligo(lactic acid)8-rapamycin prodrug (o(LA)8-RAP)-loaded poly(ethylene glycol)-block-poly(lactic acid) (PEG-b-PLA) micelle for injection, effectively increasing its water solubility to 3.3 mg/mL, and characterized its anti-tumor effects in breast tumor models.[70] However, this study did not conduct a toxicity study on the drug-loaded micelles, and the drug-loaded micelles were not used in an RCC model. Currently, there is still a lack of research on the application of nanocarriers of TEM or other mTOR inhibitors in RCC models. Our pH-responsive TEM block copolymer micelles can be considered to achieve passive tumor-targeting delivery capabilities, demonstrating excellent safety and effectiveness, and represent a material with great potential in clinical cancer therapy.

Conclusion

In conclusion, we constructed a pH-responsive TEM-loaded micelles, which serves as a potential breakthrough for TEM therapy in RCC. mPEG-PBAE, as an amphiphilic block copolymer drug delivery carrier, self-assembled under surface tension to form spherical nanoparticles in aqueous solution. TEM loaded inside the nanoparticles forms a hydrophobic core, which ultimately improves the drug solubility problem. We tried to adjust the polymerization degree of mPEG-PBAE amphiphilic block copolymer to make the pH response range of the polymer match the pH of the tumor microenvironment, and finally optimized the polymer pH response range of 6.5–7.5 when the polymerization degree of the hydrophobic segments was 5. The in vitro release rate and the polymer characterization results confirmed the controlled release of TEM delivered by mPEG-PBAE. In addition, we evaluated the TEM-loaded micelles and showed that mPEG-PBAE showed hemolytic effect at 100 μg/

mL, and compared with the same concentration of free TEM, TEM delivered by mPEG-PBAE showed better tumor inhibition and safety. The increased concentration of TEM inside the tumor and the promotion of cellular uptake may be the key factors for the enhanced antitumor activity of mPEG-PBAE nanomicelles. This study has some limitations: The HPLC detection method of TEM developed is only suitable for quantification and prescription optimization in this study. This method has a large error in terms of durability, and the conditions need to be further optimized in the future. Moreover, the enhanced permeability and retention (EPR) effect on solid tumors, although observable in vitro, still requires further research to evaluate its effectiveness in vivo. Hence, this TEM-loaded micelles as a promising and ideal therapeutic agent. Together, these results emphasize the importance of further studying the clinical utility of these particles in future studies, promising extensive applications in the medical field.

Abbreviations

RCC, renal cell carcinoma; mRCC, metastatic renal cell carcinoma; TEM, temsirolimus; mPEG-PBAE, poly(ethylene glycol) monomethyl ether-poly(beta-amino ester); nccRCC, non-clear cell RCC; EE, entrapment efficiency; EPR, enhanced permeability and retention; mTOR, mammalian target of rapamycin; VEGFR-TKI, Vascular endothelial growth factor receptor-tyrosine kinase inhibitors; PMs, polymeric micelles; ACN, Acetonitrile; MeOH, methanol; 1,6-HDDA, 1,6-hexanediol diacrylate; TFA, trifluoroacetic acid; DMSO, Dimethyl sulfoxide; PBS, phosphate-buffered solution; FBS, fetal bovine serum; CCK-8, Cell Counting Kit-8; CMC, critical micelle concentration; HPLC, High Performance Liquid Chromatography; DAD, diode-array detector; LOD, limit of detection; LOQ, limit of quantification; TCM, trichloromethane; DLS, Dynamic light scattering; FID, flame ionization detector; ALT, alanine aminotransferase; AST, aspartate transaminase; Cr, creatinine; BUN, blood urea nitrogen; NS, normal saline; PDI, polydispersity indexes; GRAS, Generally Recognized as Safe; FDA, Food and Drug Administration; P-gp, P-glycoprotein.

Ethical and Legal Approval

All protocols followed in the animal experiments were approved by the Experimental Animal Welfare and Ethics Committee of Fujian Provincial Hospital and in accordance with the principles of "Guide for the Care and Use of Laboratory Animals" and "The Guidance to Experimental Animal Welfare and Ethical Treatment" established by the National Science Council of China. All efforts were made to minimize animal suffering.

Acknowledgments

The authors would like to thank the National Natural Science Foundation of Fujian, China (No.2023J011188).

Author Contributions

All authors made a significant contribution to the work reported, whether that is in the conception, study design, execution, acquisition of data, analysis, and interpretation, or in all these areas; took part in drafting, revising or critically reviewing the article; gave final approval of the version to be published; have agreed on the journal to which the article has been submitted; and agree to be accountable for all aspects of the work.

Funding

Supported by a grant from the National Natural Science Foundation of Fujian, China (No.2023J011188).

Disclosure

The authors report no conflicts of interest in this work.

References

1. Wiechno P, Kucharz J, Sadowska M, et al. Contemporary treatment of metastatic renal cell carcinoma. *Med Oncol*. 2018;35(12):156. doi:10.1007/s12032-018-1217-1

2. Zibelman M, Barth P, Handorf E, et al. A review of interventional clinical trials in renal cell carcinoma: a status report from the Clinicaltrials.gov WebSite. *Clin Genitourin Cancer*. 2015;13(2):142–149. doi:10.1016/j.clgc.2014.08.005
3. Chen YW, Wang L, Panian J, et al. Treatment landscape of renal cell carcinoma. *Curr Treat Options Oncol*. 2023;24(12):1889–1916. doi:10.1007/s11864-023-01161-5
4. Gore ME, Szczylik C, Porta C, et al. Final results from the large sunitinib global expanded-access trial in metastatic renal cell carcinoma. *Br J Cancer*. 2015;113(1):12–19. doi:10.1038/bjc.2015.196
5. Hong MH, Kim HS, Kim C, et al. Treatment outcomes of sunitinib treatment in advanced renal cell carcinoma patients: a single cancer center experience in Korea. *Cancer Res Treat*. 2009;41(2):67–72. doi:10.4143/crt.2009.41.2.67
6. Stadler WM, Figlin RA, McDermott DF, et al. Safety and efficacy results of the advanced renal cell carcinoma sorafenib expanded access program in North America. *Cancer*. 2010;116(5):1272–1280. doi:10.1002/cncr.24864
7. Stadler WM, Figlin RA, Ernstoff MS, et al. The Advanced Renal Cell Carcinoma Sorafenib (ARCCS) expanded access trial: safety and efficacy in patients (pts) with non-clear cell (NCC) renal cell carcinoma (RCC). *J Clin Oncol*. 2007;25(18 Suppl):5036. doi:10.1200/jco.2007.25.18_suppl.5036
8. Hudes G, Carducci M, Tomczak P, et al. Temsirolimus, interferon alfa, or both for advanced renal-cell carcinoma. *N Engl J Med*. 2007;356(22):2271–2281. doi:10.1056/NEJMoa066838
9. Dutcher JP, de Souza P, McDermott D, et al. Effect of temsirolimus versus interferon-alpha on outcome of patients with advanced renal cell carcinoma of different tumor histologies. *Med Oncol*. 2009;26(2):202–209. doi:10.1007/s12032-009-9177-0
10. Tannir NM, Jonasch E, Albiges L, et al. Everolimus versus sunitinib prospective evaluation in metastatic non-clear cell renal cell carcinoma (ESPN): a randomized multicenter Phase 2 trial. *Eur Urol*. 2016;69(5):866–874. doi:10.1016/j.eururo.2015.10.049
11. Armstrong AJ, Broderick S, Eisen T, et al. Final clinical results of a randomized Phase II international trial of everolimus vs. sunitinib in patients with metastatic non-clear cell renal cell carcinoma (ASPEN). *J Clin Oncol*. 2015;33(15 Suppl):4507. doi:10.1200/jco.2015.33.15_suppl.4507
12. Hay N, Sonenberg N. Upstream and downstream of mTOR. *Genes Dev*. 2004;18(16):1926–1945. doi:10.1101/gad.1212704
13. Hua H, Kong Q, Zhang H, et al. Targeting mTOR for cancer therapy. *J Hematol Oncol*. 2019;12(1):71. doi:10.1186/s13045-019-0754-1
14. Di Lorenzo G, Buonerba C, Federico P, et al. Third-line sorafenib after sequential therapy with sunitinib and mTOR inhibitors in metastatic renal cell carcinoma. *Eur Urol*. 2010;58(6):906–911. doi:10.1016/j.eururo.2010.09.008
15. Grünwald V, Weikert S, Seidel C, et al. Efficacy of sunitinib re-exposure after failure of an mTOR inhibitor in patients with metastatic RCC. *Onkologie*. 2011;34(6):310–314. doi:10.1159/000328575
16. Hall MN. TOR and paradigm change: cell growth is controlled. *Mol Biol Cell*. 2016;27(18):2804–2806. doi:10.1091/mbc.e15-05-0311
17. Motzer RJ, Hudes GR, Curti BD, et al. Phase I/II trial of temsirolimus combined with interferon alfa for advanced renal cell carcinoma. *J Clin Oncol*. 2007;25(25):3958–3964. doi:10.1200/JCO.2006.10.5916
18. Pantuck AJ, Seligson DB, Klatte T, et al. Prognostic relevance of the mTOR pathway in renal cell carcinoma: implications for molecular patient selection for targeted therapy. *Cancer*. 2007;109(11):2257–2267. doi:10.1002/cncr.22677
19. Vonarbourg A, Passirani C, Saulnier P, et al. Parameters influencing the stealthiness of colloidal drug delivery systems. *Biomaterials*. 2006;27(24):4356–4373. doi:10.1016/j.biomaterials.2006.03.039
20. Zhang J, Li J, Shi Z, et al. pH-sensitive polymeric nanoparticles for co-delivery of doxorubicin and curcumin to treat cancer via enhanced pro-apoptotic and anti-angiogenic activities. *Acta Biomater*. 2017;58:349–364. doi:10.1016/j.actbio.2017.04.029
21. Deprimo SE, Bello CL, Smeraglia J, et al. Circulating protein biomarkers of pharmacodynamic activity of sunitinib in patients with metastatic renal cell carcinoma: modulation of VEGF and VEGF-related proteins. *J Transl Med*. 2007;5(1):32. doi:10.1186/1479-5876-5-32
22. Ness DB, Pooler DB, Ades S, et al. A phase II study of alternating sunitinib and temsirolimus therapy in patients with metastatic renal cell carcinoma. *Cancer Med*. 2023;12(12):13100–13110. doi:10.1002/cam4.5990
23. Kobayashi Y, Yamada D, Kawai T, et al. Different immunological effects of the molecular targeted agents sunitinib, everolimus and temsirolimus in patients with renal cell carcinoma. *Int J Oncol*. 2020;56(4):999–1013.
24. Cyphert EL, von Recum HA, Yamato M, et al. Surface sulfonamide modification of poly(N-isopropylacrylamide)-based block copolymer micelles to alter pH and temperature responsive properties for controlled intracellular uptake. *J Biomed Mater Res A*. 2018;106(6):1552–1560. doi:10.1002/jbm.a.36356
25. Ghasemi S, Ahmadi L, Farjadian F. Thermo-responsive PNIPAAm-b-PLA amphiphilic block copolymer micelle as nanoplatform for docetaxel drug release. *J Mater Sci*. 2022;57(36):17433–17447. doi:10.1007/s10853-022-07711-w
26. Kou Z, Dou D, Mo H, et al. Preparation and application of a polymer with pH/temperature-responsive targeting. *Int J Biol Macromol*. 2020;165(Pt A):995–1001. doi:10.1016/j.ijbiomac.2020.09.248
27. Wang T, Wu C, Hu Y, et al. Stimuli-responsive nanocarrier delivery systems for Pt-based antitumor complexes: a review. *RSC Adv*. 2023;13(24):16488–16511. doi:10.1039/D3RA00866E
28. Li Y, Leng M, Cai M, et al. pH responsive micelles based on copolymers mPEG-PCL-PDEA: the relationship between composition and properties. *Colloids Surf B Biointerfaces*. 2017;154:397–407. doi:10.1016/j.colsurfb.2017.03.045
29. Kalhapure RS, Renukuntla J. Thermo- and pH dual responsive polymeric micelles and nanoparticles. *Chem Biol Interact*. 2018;295:20–37. doi:10.1016/j.cbi.2018.07.016
30. Wu H, Dong J, Li C, et al. Multi-responsive nitrobenzene-based amphiphilic random copolymer assemblies. *Chem Commun*. 2013;49(34):3516–3518. doi:10.1039/c3cc39043h
31. Hsu CW, Hsieh MH, Xiao MC, et al. pH-responsive polymeric micelles self-assembled from benzoic-imine-containing alkyl-modified PEGylated chitosan for delivery of amphiphilic drugs. *Int J Biol Macromol*. 2020;163:1106–1116. doi:10.1016/j.ijbiomac.2020.07.110
32. Porrang S, Rahemi N, Davaran S, et al. Preparation and in-vitro evaluation of mesoporous biogenic silica nanoparticles obtained from rice and wheat husk as a biocompatible carrier for anti-cancer drug delivery. *Eur J Pharm Sci*. 2021;163:105866. doi:10.1016/j.ejps.2021.105866
33. Tan L, Fan J, Zhou Y, et al. Preparation of reversible cross-linked amphiphilic polymeric micelles with pH-responsive behavior for smart drug delivery[J]. *RSC Adv*. 2023;13(40):28165–28178. doi:10.1039/D3RA05575B
34. Yu C, Wang L, Xu Z, et al. Smart micelles self-assembled from four-arm star polymers as potential drug carriers for pH-triggered DOX release[J]. *J Polym Res*. 2020;27(5):1–10. doi:10.1007/s10965-020-02108-2
35. Li Y, Niu Y, Hu D, et al. Preparation of light-responsive polyester micelles via ring-opening polymerization of o-carboxyanhydride and azide–alkyne click chemistry[J]. *Macromol Chem Phys*. 2015;216(1):77–84. doi:10.1002/macp.201400406

36. Zhang Y, Zhang X, Chen W, et al. Self-assembled micelle responsive to quick NIR light irradiation for fast drug release and highly efficient cancer therapy. *J Control Release*. 2021;336:469–479. doi:10.1016/j.jconrel.2021.06.028
37. Yap JE, Zhang L, Lovegrove JT, et al. Visible light-responsive drug delivery nanoparticle via Donor-Acceptor Stenhouse Adducts (DASA). *Macromol Rapid Commun*. 2020;41(21):e2000236. doi:10.1002/marc.202000236
38. Zhao Y, Tavares AC, Gauthier MA. Nano-engineered electro-responsive drug delivery systems. *J Mater Chem B*. 2016;4(18):3019–3030. doi:10.1039/C6TB00049E
39. Kalafatovic D, Nobis M, Javid N, et al. MMP-9 triggered micelle-to-fibre transitions for slow release of doxorubicin. *Biomater Sci*. 2015;3 (2):246–249. doi:10.1039/C4BM00297K
40. Slor G, Tevet S, Amir RJ. Stimuli-induced architectural transition as a tool for controlling the enzymatic degradability of polymeric micelles. *ACS Polym Au*. 2022;2(5):380–386. doi:10.1021/acspolymersau.2c00023
41. Barve A, Jain A, Liu H, et al. Enzyme-responsive polymeric micelles of cabazitaxel for prostate cancer targeted therapy. *Acta Biomater*. 2020;113:501–511. doi:10.1016/j.actbio.2020.06.019
42. Wang Y, Song W, Bao L, et al. Enzyme and pH dual responsive linear-dendritic block copolymer micelles based on a phenylalanyl-lysine motif and peripherally ketal-functionalized dendron as potential drug carriers. *RSC Adv*. 2023;13(32):22079–22087. doi:10.1039/D3RA03790H
43. Zhou H, Qi Z, Xue X, et al. Novel pH-sensitive urushiol-loaded polymeric micelles for enhanced anticancer activity. *Int J Nanomed*. 2020;15:3851–3868. doi:10.2147/IJN.S250564
44. Liu L, Venkatraman SS, Yang YY, et al. Polymeric micelles anchored with TAT for delivery of antibiotics across the blood-brain barrier. *Biopolymers*. 2008;90(5):617–623. doi:10.1002/bip.20998
45. Zhao YZ, Sun CZ, Lu CT, et al. Characterization and anti-tumor activity of chemical conjugation of doxorubicin in polymeric micelles (DOX-P) in vitro. *Cancer Lett*. 2011;311(2):187–194. doi:10.1016/j.canlet.2011.07.013
46. La SB, Okano T, Kataoka K. Preparation and characterization of the micelle-forming polymeric drug indomethacin-incorporated poly(ethylene oxide)-poly(beta-benzyl L-aspartate) block copolymer micelles. *J Pharm Sci*. 1996;85(1):85–90. doi:10.1021/js950204r
47. Zhao L, Du J, Duan Y, et al. Curcumin loaded mixed micelles composed of Pluronic P123 and F68: preparation, optimization and in vitro characterization. *Colloids Surf B Biointerfaces*. 2012;97:101–108. doi:10.1016/j.colsurfb.2012.04.017
48. Bae KH, Choi SH, Park SY, et al. Thermosensitive pluronic micelles stabilized by shell cross-linking with gold nanoparticles. *Langmuir*. 2006;22 (14):6380–6384. doi:10.1021/la0606704
49. Gong J, Huo M, Zhou J, et al. Synthesis, characterization, drug-loading capacity and safety of novel octyl modified serum albumin micelles. *Int J Pharm*. 2009;376(1–2):161–168. doi:10.1016/j.ijpharm.2009.04.033
50. Zhou Q, Zhang Z, Chen T, et al. Preparation and characterization of thermosensitive pluronic F127-b-poly(ε-caprolactone) mixed micelles. *Colloids Surf B Biointerfaces*. 2011;86(1):45–57. doi:10.1016/j.colsurfb.2011.03.013
51. Ge H, Hu Y, Jiang X, et al. Preparation, characterization, and drug release behaviors of drug nimodipine-loaded poly(epsilon-caprolactone)-poly (ethylene oxide)-poly(epsilon-caprolactone) amphiphilic triblock copolymer micelles. *J Pharm Sci*. 2002;91(6):1463–1473. doi:10.1002/jps.10143
52. Kulthe SS, Inamdar NN, Choudhari YM, et al. Mixed micelle formation with hydrophobic and hydrophilic Pluronic block copolymers: implications for controlled and targeted drug delivery. *Colloids Surf B Biointerfaces*. 2011;88(2):691–696. doi:10.1016/j.colsurfb.2011.08.002
53. Koppel DE. Analysis of macromolecular polydispersity in intensity correlation spectroscopy: the method of cumulants[J]. *J Chem Phys*. 1972;57 (11):4814–4820. doi:10.1063/1.1678153
54. Damodaran VB, Fee CJ, Ruckh T, et al. Conformational studies of covalently grafted poly(ethylene glycol) on modified solid matrices using X-ray photoelectron spectroscopy. *Langmuir*. 2010;26(10):7299–7306. doi:10.1021/la9041502
55. Firouzi S, Haghighatdoost F. The effects of prebiotic, probiotic, and synbiotic supplementation on blood parameters of renal function: a systematic review and meta-analysis of clinical trials. *Nutrition*. 2018;51–52:104–113. doi:10.1016/j.nut.2018.01.007
56. Cai H, Su S, Li Y, et al. Protective effects of Salvia miltiorrhiza on adenine-induced chronic renal failure by regulating the metabolic profiling and modulating the NADPH oxidase/ROS/ERK and TGF-β/Smad signaling pathways. *J Ethnopharmacol*. 2018;212:153–165. doi:10.1016/j.jep.2017.09.021
57. Pradeep K, Ko KC, Choi MH, et al. Protective effect of hesperidin, a citrus flavanoglycone, against γ-radiation-induced tissue damage in Sprague-Dawley rats. *J Med Food*. 2012;15(5):419–427. doi:10.1089/jmf.2011.1737
58. Gong N, Zhang Y, Teng X, et al. Proton-driven transformable nanovaccine for cancer immunotherapy. *Nat Nanotechnol*. 2020;15(12):1053–1064. doi:10.1038/s41565-020-00782-3
59. Li C, Zhou J, Wu Y, et al. Core role of hydrophobic core of polymeric nanomicelle in endosomal escape of siRNA. *Nano Lett*. 2021;21 (8):3680–3689. doi:10.1021/acs.nanolett.0c04468
60. Gao GH, Li Y, Lee DS. Environmental pH-sensitive polymeric micelles for cancer diagnosis and targeted therapy. *J Control Release*. 2013;169 (3):180–184. doi:10.1016/j.jconrel.2012.11.012
61. Tirosh O, Barenholz Y, Katzhendler J, et al. Hydration of polyethylene glycol-grafted liposomes. *Biophys J*. 1998;74(3):1371–1379. doi:10.1016/S0006-3495(98)77849-X
62. Branca C, Magazu S, Maisano G, et al. Hydration study of PEG/water mixtures by quasi elastic light scattering, acoustic and rheological measurements[J]. *J Phys Chem A*. 2002;106(39):10272–10276. doi:10.1021/jp014345v
63. Jeon SI, Lee JH, Andrade JD, et al. Protein—surface interactions in the presence of polyethylene oxide: i. Simplified theory[J]. *J Colloid Interface Sci*. 1991;142(1):149–158. doi:10.1016/0021-9797(91)90043-8
64. Lasic DD, Martin FJ, Gabizon A, et al. Sterically stabilized liposomes: a hypothesis on the molecular origin of the extended circulation times. *Biochim Biophys Acta*. 1991;1070(1):187–192. doi:10.1016/0005-2736(91)90162-2
65. Needham D, McIntosh TJ, Lasic DD. Repulsive interactions and mechanical stability of polymer-grafted lipid membranes. *Biochim Biophys Acta*. 1992;1108(1):40–48. doi:10.1016/0005-2736(92)90112-Y
66. Sharma S, Johnson RW, Desai TA. XPS and AFM analysis of antifouling PEG interfaces for microfabricated silicon biosensors. *Biosens Bioelectron*. 2004;20(2):227–239. doi:10.1016/j.bios.2004.01.034
67. Su Z, Liang Y, Yao Y, et al. Polymeric complex micelles based on the double-hydrazone linkage and dual drug-loading strategy for pH-sensitive docetaxel delivery. *J Mater Chem B*. 2016;4(6):1122–1133. doi:10.1039/C5TB02188J

68. Zhang L, Lu J, Jin Y, et al. Folate-conjugated beta-cyclodextrin-based polymeric micelles with enhanced doxorubicin antitumor efficacy. *Colloids Surf B Biointerfaces*. 2014;122:260–269. doi:10.1016/j.colsurfb.2014.07.005
69. Cai H, Zheng R, Wu N, et al. Chimeric peptide engineered nanomedicine for synergistic suppression of tumor growth and therapy-induced hyperlipidemia by mTOR and PCSK9 inhibition. *Pharmaceutics*. 2023;15(10):2377. doi:10.3390/pharmaceutics15102377
70. Tam YT, Repp L, Ma Z-X, et al. Oligo(Lactic Acid)8-Rapamycin Prodrug-Loaded Poly(Ethylene Glycol)-block-Poly(Lactic Acid) Micelles for Injection. *Pharm Res*. 2019;36(5):70. doi:10.1007/s11095-019-2600-0